

Article

Reflectance Spectral Characteristics of Minerals in the Mboukoumassi Sylvite Deposit, Kouilou Province, Congo

Xian-Fu Zhao ^{1,2}, Zong-Qi Wang ^{1,*}, Jun-Ting Qiu ^{3,*} and Yang Song ²

¹ Ministry of Land and Resources Key Laboratory of Metallogeny and Mineral Assessment, Institute of Mineral Resources, Chinese Academy of Geological Sciences, Beijing 100037, China; zhzy-zhaoxf@avic-intl.cn

² School of Earth Sciences and Resources, China University of Geosciences, Beijing 100083, China; daodanjiayou@gmail.com

³ National Key Laboratory of Science and Technology on Remote Sensing Information and Image Analysis, Beijing Research Institute of Uranium Geology, Beijing 100029, China

* Correspondence: kcwangzongqi@gmail.com (Z.-Q.W.); qiu junting@cugb.edu.cn (J.-T.Q.); Tel.: +86-10-82251207 (Z.-Q.W.); +86-10-64962683 (J.-T.Q.)

Academic Editor: Dimitrina Dimitrova

Received: 20 March 2016; Accepted: 23 May 2016; Published: 14 June 2016

Abstract: This study presents reflectance spectra, determined with an ASD Inc. TerraSpec[®] spectrometer, of five types of ore and gangue minerals from the Mboukoumassi sylvite deposit, Democratic Republic of the Congo. The spectral absorption features, with peaks at 999, 1077, 1206, 1237, 1524, and 1765 nm, of the ore mineral carnallite were found to be different from those of gangue minerals. Spectral comparison among carnallite samples from different sylvite deposits suggests that, in contrast to spectral shapes, the absorption features of carnallite are highly reproducible. Heating of carnallite to 400 and 750°C, and comparing the spectra of heated and non-heated samples, indicates that spectral absorption is related to lattice hydration or addition of hydroxyl. Since carnallite undergoes deliquescence easily, the absorption features of carnallite in the 350–2500 nm spectrum could serve as a robust tool for carnallite identification and separation.

Keywords: reflectance spectrum; mineral classification and separation; sylvite deposit; Mboukoumassi; Congo

1. Introduction

Potassium, a common soil fertilizer, is important for modern agriculture as it improves water retention, nutrient value, and disease resistance of food crops. Often referred to as potash, most industrial potassium is derived from sylvite deposits, including those in Canada, Russia, China, Belarus, Israel, Germany, Chile, the United States, Jordan, Spain, the United Kingdom, and Brazil. Potash ores are typically rich in potassium chloride (KCl) and sodium chloride (NaCl), and are often buried deep below the Earth's surface. Extraction of potash ore is typically by conventional shaft mining with the extracted ore ground into grains.

Carnallite ($\text{KCl} \cdot \text{MgCl}_2 \cdot 6\text{H}_2\text{O}$), a key potassium-bearing mineral used for potassium production, is usually spatially associated with halite, a common gangue mineral in carnallite ore. The occurrence of halite may reduce the economic benefit of sylvite and increase difficulties during potassium purification. Therefore, to improve processing efficiency, it is necessary to determine halite content and distinguish carnallite from gangue minerals. Traditional geochemical methods for halite content estimation are limited because analyzed samples are typically collected discontinuously from drill cores, and the dissolution method for separating carnallite from halite is time-consuming and uneconomic.

Hyperspectral remote sensing, which has been successfully used in lithological classification [1–5] and alteration mineral identification [6–8], provides a potential alternative for halite estimation and carnallite separation in the solid state. Materials that interact with the electromagnetic waves emitted from the sun can be recorded by hyperspectral sensors in the form of a spectrum. A spectrum can essentially fingerprint a material; it can be used to search for material with a similar spectrum and to investigate the composition of the material [9].

In this study, the reflectance spectra (350–2500 nm) of several mineral samples (anhydrite, glauberite, halite, carnallite, and tachydrite) were recorded from the Mboukoumassi sylvite deposit, Kouilou Province, Democratic Republic of the Congo. This was done using an ASD Inc. (Boulder, CO, USA) TerraSpec® spectrometer in an attempt to understand the spectral features of these minerals and evaluate the capability of hyperspectral remote sensing technology in identification and classification of minerals in the sylvite deposit.

2. Geological Backgrounds

The Mboukoumassi deposit in the southwest of Kouilou Province in the Democratic Republic of the Congo is an important potash and halite deposit in the Congo Basin (Figure 1). The deposit is hosted in Cretaceous strata and covered by Quaternary sediments. The Cretaceous sedimentary strata consist of basal continental sedimentary rocks, a middle stratum of rock salt, and a capping of marine sedimentary rocks. The continental sedimentary rocks were formed before or coeval with the formation of the African-American continent rift. The rock salt layer bears light pink, salmon-colored and dark salmon colored carnallite, bluish white to steel gray or light brown halite, bischofite, and tachydrite. This unit is composed of four sedimentary cyclothems, with bischofite and tachydrite in the top layer, and bituminous shale (or asphaltene-halite) in the bottom layer. The rock salt layer thickens from the edges to the center of the basin, with thickness in the range of 170–600 m. The marine sedimentary rocks were deposited at the edge of the then African continental margin and differ from most other marine deposits because it lacks sulfates and carbonates.

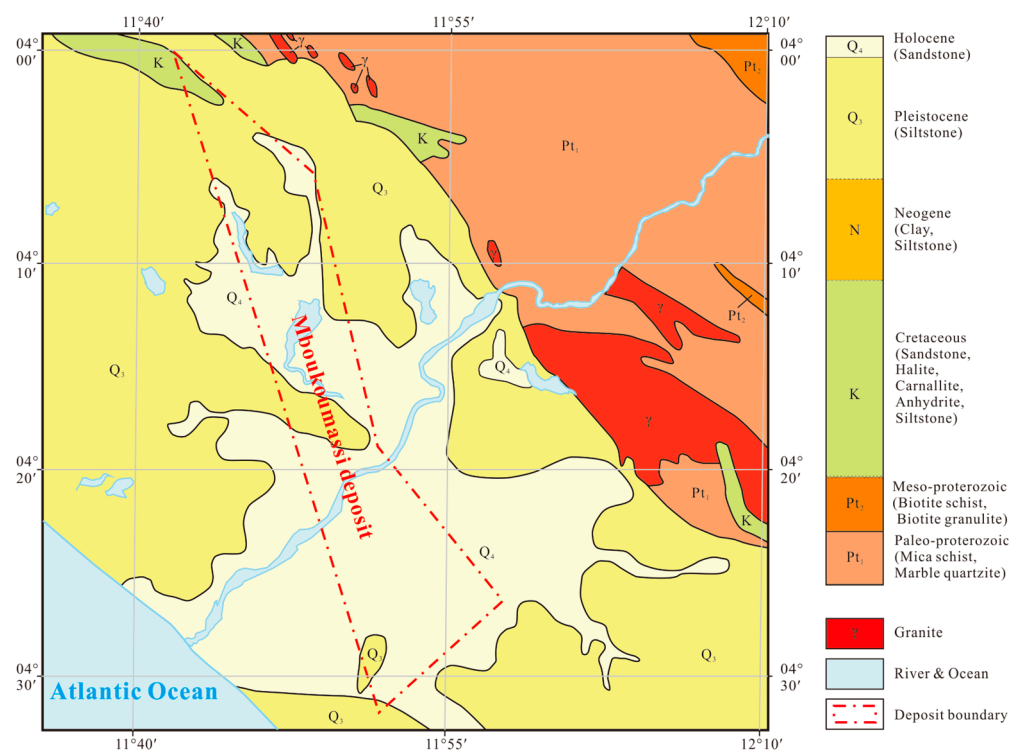


Figure 1. Geological map for Mboukoumassi deposit (Modified after Martiniand Bowles (1994) [10]).

During the Cretaceous Period, the Mboukoumassi deposit was located in a rift basin where tectonic movements were lacking, resulting in negligible deformation. This is evident from the horizontal and highly continuous deposit, and its uniform thickness. Only minor small faults and some caverns can be found in the strata.

The dominant ore minerals in the Mboukoumassi deposit are carnallite and potassium-halite. The potassium-halite ore bodies are discontinuous and are lenticular in shape, as opposed to the stratiform and continuous carnallite ore bodies. The gangue minerals include halite, anhydrite, bischofite, tachydrite, plus minor amounts of dolomite, calcite, and clay. The ore-bearing stratum is mainly composed of carnallite and halite interbeds, where bituminous shale and bischofite are developed. The total average thickness of strata that hosts ore bodies is 259.61 m.

3. Samples and Analytical Methods

The mineral samples analyzed in this study were collected from drill cores BS-3 and ZK143. The photographs of individual representative samples are shown in Figure 2, and the location and physical properties of the samples are given in Table 1. The elemental compositions of these samples (Table 2) were determined using atomic absorption at the Chinese Academy of Geological Sciences.

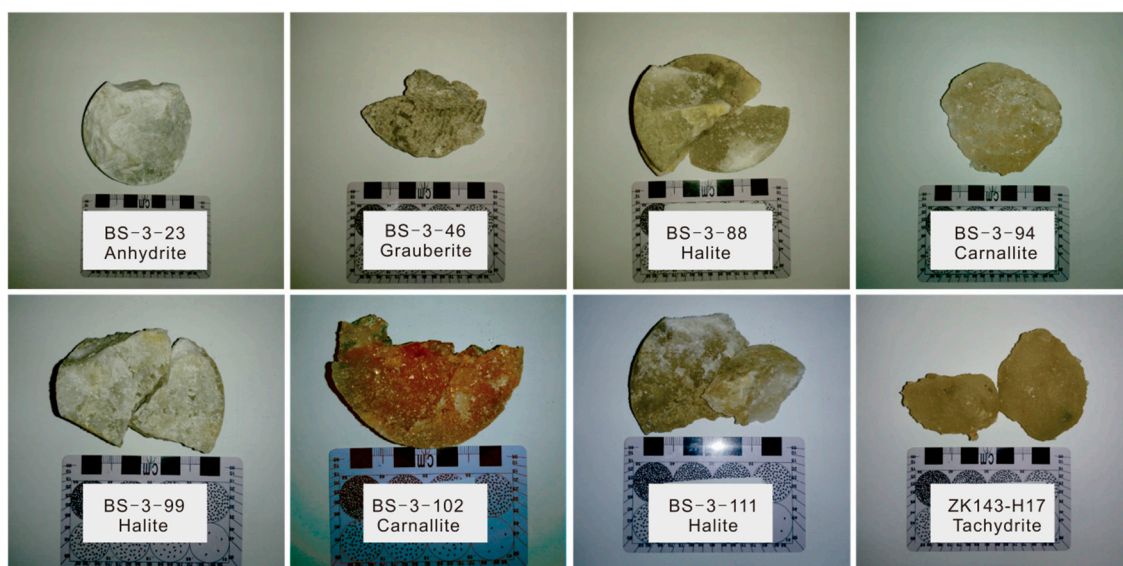


Figure 2. Photographs of the mineral samples from the Mboukoumassi deposit, Kouilou Province, Congo.

Table 1. Sample location, lithology, and mineral descriptions; Mboukoumassi deposit, Kouilou Province, Congo.

Sample No.	Lithology	Location ¹	Description
BS-3-23	Anhydrite	D.C. BS-3 –240.80 m	White or gray in color, opaque, blocky structure, earthy luster
BS-3-46	Grauberite	D.C. BS-3 –308.10 m	Gray in color, opaque, blocky structure, earthy luster
BS-3-88	Halite	D.C. BS-3 –447.31 m	Gray in color, translucent, fine to medium grained, blocky structure, vitreous to earthy luster
BS-3-94	Carnallite	D.C. BS-3 –453.71 m	Lightpink in color, translucent, blocky structure, oily luster
BS-3-99	Halite	D.C. BS-3 –464.73 m	Gray to white in color, translucent, blocky structure, vitreous to earthy luster

Table 1. Cont.

Sample No.	Lithology	Location ¹	Description
BS-3-102	Carnallite	D.C. BS-3 –474.55 m	Salmon to darksalmon in color, translucent, blocky structure, oily luster
BS-3-111	Halite	D.C. BS-3 –494.19 m	Gray in color, translucent, blocky structure, vitreous to earthy luster
ZK143-H17	Tachydrate	D.C. ZK143 –435.00 m	Goldenrod in color, translucent, oily luster, very soluble

¹ Note: D.C. = Drilling Core.

The spectra of mineral samples from the Mboukoumassi deposit were measured using an ASD Inc. TerraSpec[®] spectrometer at the China National Key Laboratory of Science and Technology on Remote Sensing Information and Image Analysis (NKLST-RSIIA). The technical specifications of the spectrometer are summarized in Table 3.

Table 2. Element composition (unit wt %)¹ of mineral samples from the Mboukoumassi deposit, Kouilou Province, Democratic Republic of the Congo.

Sample	Mg	K	Sr	Na	Ca	Li	B	S	Cl	Br
BS-3-23	0.1646	0.0072	0.0864	0.0666	24.9031	0.0023	0.0195	64.5483	0.1919	1.7114
BS-3-46	0.1637	0.0187	0.0665	9.3709	20.5751	0.0066	0.1195	53.2418	17.4755	2.1987
BS-3-88	0.0775	0.0928	0.0022	39.0701	0.2392	0.0002	0.0004	0.1292	60.2938	0.0456
BS-3-94	7.4666	11.3368	0.0004	6.2572	0.0557	0.0001	0.0000	0.0307	43.1870	0.4341
BS-3-99	0.3203	0.6943	0.0025	36.3044	0.4268	0.0001	0.0029	0.2901	59.4677	0.0590
BS-3-102	6.6710	10.9012	0.0005	8.3753	0.0657	0.0000	0.0000	0.0385	38.7926	0.2900
BS-3-111	0.0478	0.0363	0.0021	38.2802	0.3930	0.0001	0.0010	0.2672	60.5064	0.0337
ZK143-H17	11.5903	0.3040	0.1885	0.2841	5.1510	0.0000	0.0107	0.1136	44.4799	5.7306

¹ Note: element compositions were determined using atomic absorption method at Chinese Academy of Geological Sciences.

Table 3. Technical specifications of the ASD Inc. TerraSpec[®] spectrometer.

Item	Parameter
Spectral Range	350 to 2500 nm
Spectral Resolutions	3 nm @ 700 nm 6 nm @ 1400 nm 6 nm @ 2100 nm
Sampling Intervals	1.4 nm between 350 and 1000 nm 2 nm between 1000 and 2500 nm
Signal to Noise Values	9500 DN @ 700 nm 5000 DN @ 1400 nm 800 DN @ 2100 nm

The experimental procedure proceeds as follows: the spectrometer is set up according to the Labspec4 user manual and connected to a laptop. Data are recorded and manipulated using the RS3 software package (v6.4, ASD Inc.). An accessory light source is used so that measurements can be carried out without the need for sunlight. A white reference is introduced to optimize and calibrate the instrument; the reflectance of which is automatically set to 1 by the RS3 software.

Then, the detector is carefully placed on to the samples to avoid possible influence from fluorescence arising from the environment. Two or more measurements were carried out for each sample on different parts of the sample to check for unique spectral characteristic(s). Five spectra were recorded for each measurement to monitor any variation during the measurement.

The spectrum of the white reference is measured again after the experiment to check for any significant changes of the standard spectrum. The spectra of the white reference before and after the experiment are shown in Figure 3.

The spectra of mineral samples are exported as ASCII files using RS3 and ViewSpecPro® software (v.6.2, ASD Inc.), respectively. These data are then converted into a spreadsheet file with Excel® 2007 and plotted with CorelDRAW® X5 (Corel Corporation, Ottawa, ON, Canada). The results are listed in Supplementary Materials and displayed in Figure 4. The name list of the spectral files and related mineral samples is given in Table 4.

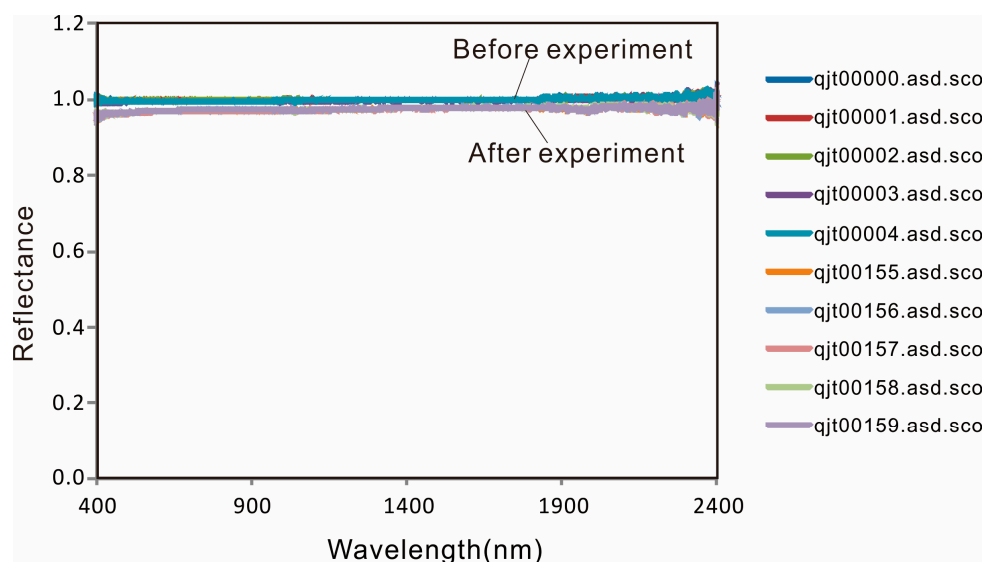


Figure 3. Spectral of white reference before and after the experiment.

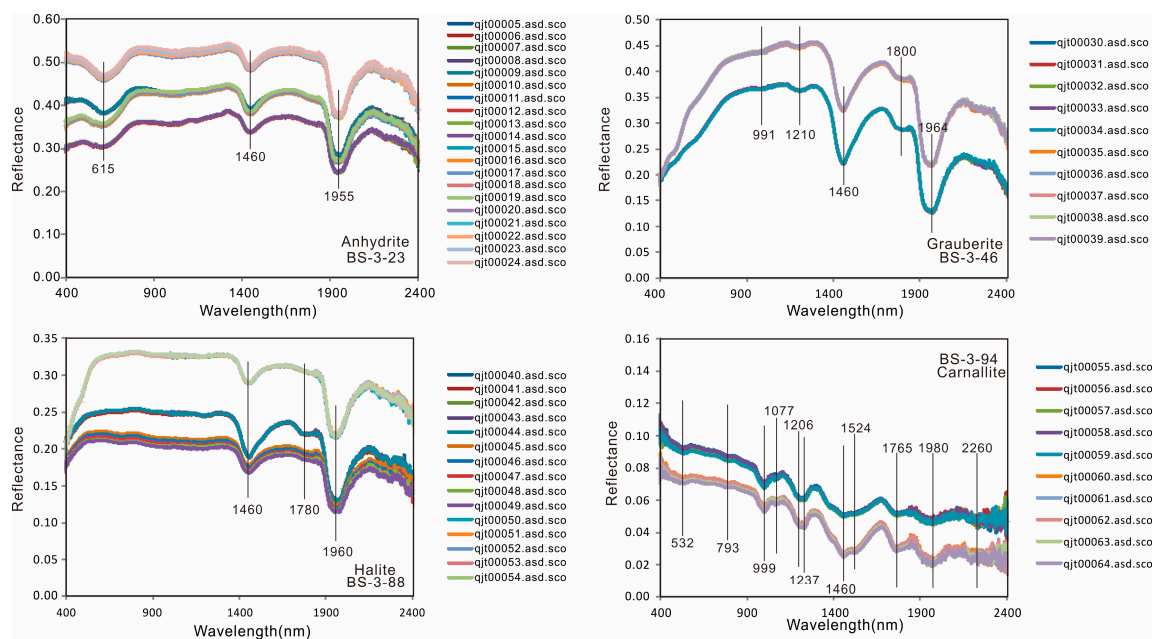


Figure 4. Cont.

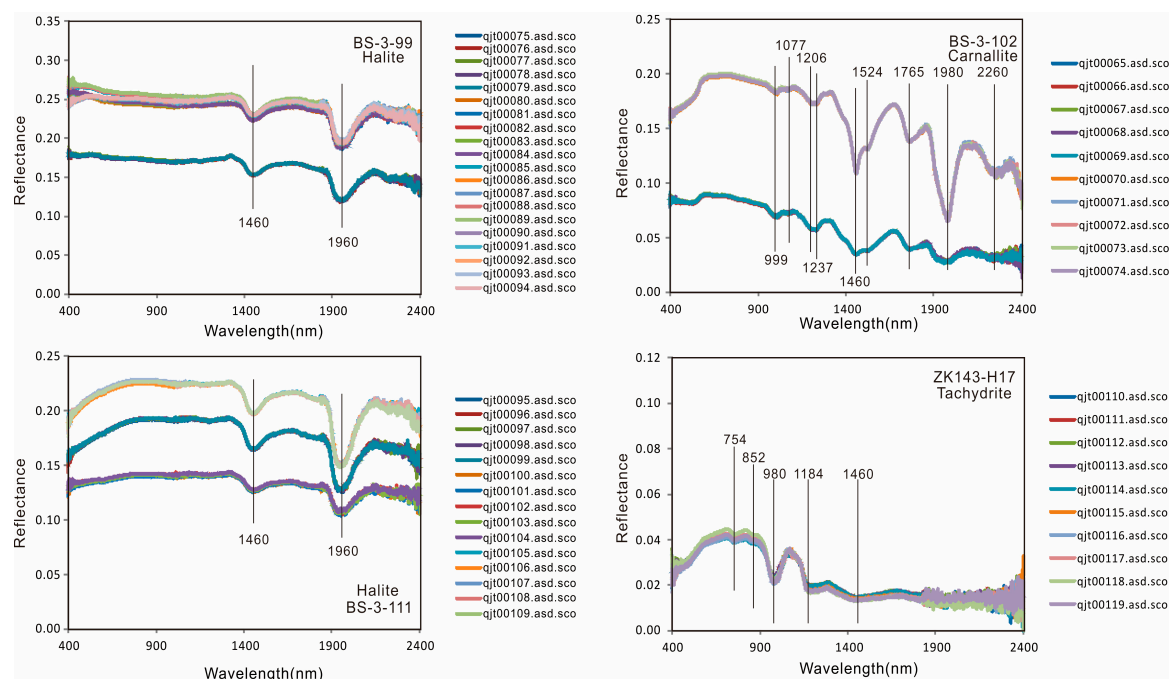


Figure 4. Spectra of eight mineral samples recorded by ASD spectrometer.

Table 4. File name list of reference and sample spectra.

File Name List	Sample No.	Comment
qjt00000.asd.sco to qjt00004.asd.sco	White Reference	Standard (1 measurement)
qjt00005.asd.sco to qjt00024.asd.sco	BS-3-23	Anhydrite (4 measurements)
qjt00030.asd.sco to qjt00039.asd.sco	BS-3-46	Grauberite (2 measurements)
qjt00040.asd.sco to qjt00054.asd.sco	BS-3-88	Halite (3 measurements)
qjt00055.asd.sco to qjt00064.asd.sco	BS-3-94	Carnallite (2 measurements)
qjt00075.asd.sco to qjt00094.asd.sco	BS-3-99	Halite (4 measurements)
qjt00065.asd.sco to qjt00074.asd.sco	BS-3-102	Carnallite (2 measurements)
qjt00095.asd.sco to qjt00109.asd.sco	BS-3-111	Halite (3 measurements)
qjt00110.asd.sco to qjt00119.asd.sco	ZK143-H17	Tachydrate (2 measurements)
qjt00155.asd.sco to qjt00159.asd.sco	White Reference	Repeat Standard (1 measurement)

4. Results

The spectra of the white reference before and after the experiment are approximately equal to 1, suggesting that no significant variation occurred during the experiment (Figure 3). The five spectra in each sample measurement are nearly identical, indicating no variation of absorption features during the measurement. This is shown in Figure 4, which displays the spectra of eight mineral samples.

Although the spectra of different parts of each mineral sample differ, they are similar in shape and show unique absorption features (Figure 4). One anhydrite sample (BS-3-23) shows absorption peaks at 615, 1460, and 1955 nm. One glauberite sample (BS-3-46) has absorption peaks at 991, 1210, 1460, 1800, and 1964 nm. Three halite samples (BS-3-88, BS-3-99, and BS-3-111) display absorption peaks at 1460 nm and 1960 nm. Two carnallite samples (BS-3-94 and BS-3-102) have absorption peaks at 999, 1077, 1206, 1237, 1460, 1524, 1765, 1980, and 2260 nm. The carnallite sample BS-3-94 also shows absorption at 532 and 793 nm. One tachydrate sample displays absorption at 754, 852, 980, 1184, and 1460 nm. All of the spectral absorption features above are listed in Table 5 and are compared with those presented in the United States Geological Survey (USGS) spectral library.

Table 5. Summary of mineral absorption peaks from this study, and reference samples from the USGS spectral library.

Mineral	Absorption(s) @ nm	Reference
BS-3-23 (Anhydrite)	615, 1460, 1955	this study
BS-3-46 (Glauberite)	991, 1210, 1460, 1800, 1964	this study
BS-3-88 (Halite)	1460, 1780, 1960,	this study
BS-3-94 (Carnallite)	532, 793, 999, 1077, 1206, 1237, 1460, 1524, 1765, 1980, 2260	this study
BS-3-99 (Halite)	1460, 1960	this study
BS-3-102 (Carnallite)	999, 1077, 1206, 1237, 1460, 1524, 1765, 1980, 2260	this study
BS-3-111 (Halite)	1460, 1960	this study
ZK143-H17 (Tachydrate)	754, 852, 980, 1184, 1460	this study
GDS42 (Anhydrite)	1464, 1955	USGS
HS433.3B (Halite)	1464, 1965	USGS
NMNH98011 (Carnallite)	1006, 1074, 1209, 1234, 1464, 1529, 1764, 1985, 2255	USGS
HS430.3B(Carnallite)	994, 1074, 1199, 1224, 1454, 1520, 1764, 1975, 2265	USGS

5. Discussion

As the dominant potassium-bearing mineral in the Mboukoumassi deposit, it is important that carnallite is distinguished from gangue minerals, such as anhydrite, glauberite, halite, and tachydrate. Since carnallite and halite have the same origin and are typically associated, it is difficult to distinguish between them and also to distinguish them from other gangue minerals. The traditional dissolution method for separating carnallite from halite is time-consuming, as is manual sorting. Which is also uneconomic. Fortunately, mineral identification based on mineral spectra provides a potential approach for solid state mineral separation. The result of this study have shown absorption peaks at 999, 1077, 1206, 1237, 1524 and 1765 nm in carnallite, which are distinct from those of halite (1660 nm), suggesting that these minerals can be distinguished using reflectance spectra.

In the Mboukoumassi deposit, two types of carnallite can be distinguished based on color: a light pink variety and a salmon- to dark salmon-colored variety (Figure 2 and Table 1). Bulk-rock geochemistry suggests that they are similar in element composition, but the red shade of the carnallite is probably due to ferric oxide inclusions [11]. The two types of carnallite have distinct spectra, but their absorptions are almost identical, except for two absorptions at 532 and 793 nm. The high degree of spectral similarity between the two carnallite varieties suggests that carnallite separation based on mineral spectral absorption is more reliable than that based on the general spectral shape.

In addition to the absorption features reported in this study, spectra of carnallites from other deposits were also collected. As shown in Figure 5a, the spectra of carnallites from Carlsbad, New Mexico [12] are also characterized by absorption peaks at 999, 1077, 1206, 1237, 1524, and 1765 nm and show high absorption reproducibility. To investigate the mechanism of these absorptions, elemental compositions of the carnallite samples from the Mboukoumassi deposit were reviewed. Samples BS-3-94 and BS-3-102 have high Na, K, Mg, and Cl contents with minor Ca, Br, and S. These elements are not critical to absorption features in the 350–2500 nm reflectance spectrum.

Since hydration of or addition of hydroxyl to the mineral may result in spectral absorptions [13] a heating experiment was carried out to investigate the relationship between carnallite spectral absorptions and hydration or hydroxyl addition. Sample BS-3-102 was powdered to 200 µm then heated to temperatures of ~400 and ~750°C in a muffle furnace. It was found that the spectral measurement for heated carnallite was the same as for raw carnallite. The spectra of sample BS-3-102 before and after heating are shown in Figure 5b; the absorption peaks of raw carnallite at 999, 1077, 1206, 1237, 1524, and 1765 nm disappeared or became weak after dehydration, suggesting that the above absorptions are related to hydration. Since carnallite undergoes deliquescence easily, the absorptions at 999, 1077, 1206, 1237, 1524, and 1765 nm may be able to be widely used as diagnostic features of carnallite and for distinguishing from halite.

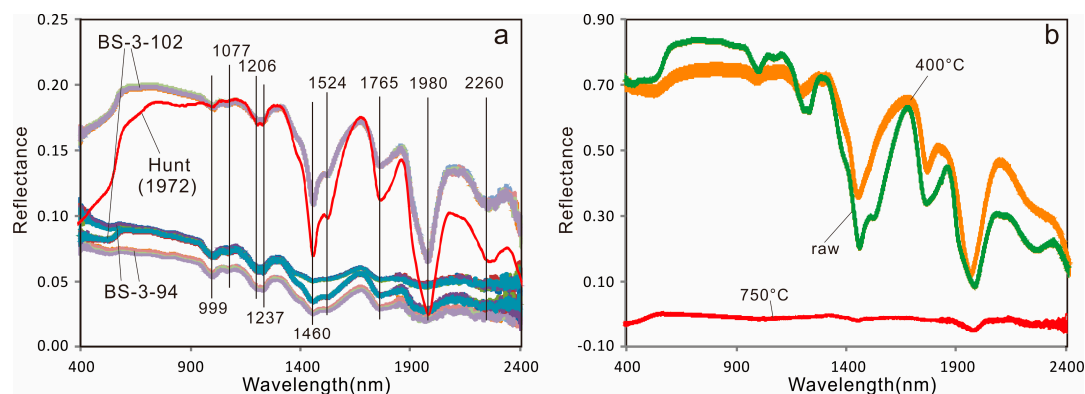


Figure 5. (a) Spectral comparison among carnallite samples BS-3-94, BS-3-102, and Hunt (1972) [12]; and (b) spectral comparison between raw and heated carnallite samples. Note that the reflectance values of the carnallite sample from Hunt (1972) [12] were divided by four for clarity.

6. Conclusions

- (1) The spectra of five main types of minerals from the Mboukoumassi deposit, Democratic Republic of the Congo, were determined: anhydrite, glauberite, halite, carnallite, and tachydrile. Anhydrite shows absorption peaks at 615, 1460, and 1955 nm. Glauberite has absorption peaks at 991, 1210, 1460, 1800, and 1964 nm. Halite displays absorption features at 1460 and 1960 nm. Carnallite has absorption peaks at 999, 1077, 1206, 1237, 1460, 1524, 1765, 1980, and 2260 nm. Tachydrile displays absorption features at 754, 852, 980, 1184, and 1460 nm.
- (2) The absorption features at 999, 1077, 1206, 1237, 1524 and 1765 nm can be used to distinguish carnallite from halite in samples and thereby assist in metallurgical extraction.
- (3) The high spectral absorption reproducibility of carnallite suggests that mineral identification based on absorption features is more reliable than that based on general spectral shape.
- (4) The absorption features of carnallite ($\text{KCl} \cdot \text{MgCl}_2 \cdot 6\text{H}_2\text{O}$) are clearly related to hydration or hydroxyl addition in its crystallographic structure, as demonstrated by the heating experiment.

Supplementary Materials: The following are available online at www.mdpi.com/2075-163X/6/2/55/s1, Original spectral file of 8 mineral samples recorded by ASD Spectrometer (Excel format).

Acknowledgments: This study was finally supported by the foundation of Sylvite Exploration Project in the Mboukoumassi deposit of Chinese Academy of Geological Sciences (ZHJS2014001) and the Youth Foundation of Beijing Research Institute of Uranium Geology (DD1405-A).

Author Contributions: Xian-Fu Zhao, Jun-Ting Qiu, and Yang Song wrote this paper. Jun-Ting Qiu measured the spectra of 8 mineral samples from the Mboukoumassi sylvite deposit. The whole paper was finally checked by Zong-Qi Wang.

Conflicts of Interest: The authors declare no conflict of interest.

References

1. Chabrilat, S.; Pinet, P.C.; Ceuleneer, G.; Johnson, P.E.; Mustard, J.F. Ronda peridotite massif: Methodology for its geological mapping and lithological discrimination from airborne hyperspectral data. *Int. J. Remote Sens.* **2000**, *21*, 2363–2388. [CrossRef]
2. Chen, X.; Warner, T.A.; Campagna, D.J. Integrating visible, near-infrared and short-wave infrared hyperspectral and multispectral thermal imagery for geological mapping at Cuprite, Nevada: A rule-based system. *Int. J. Remote Sens.* **2010**, *31*, 1733–1752. [CrossRef]
3. Harris, J.R.; McGregor, R.; Budkewitsch, P. Geological analysis of hyperspectral data over southwest Baffin Island: Methods for producing spectral maps that relate to variations in surface lithologies. *Can. J. Remote Sens.* **2010**, *36*, 412–435. [CrossRef]

4. Slavinski, H.; Morris, B.; Ugalde, H.; Spicer, B.; Skulski, T.; Rogers, N. Integration of lithological, geophysical, and remote sensing information: A basis for remote predictive geological mapping of the Baie Verte Peninsula, Newfoundland. *Can. J. Remote Sens.* **2010**, *36*, 99–118. [[CrossRef](#)]
5. Qiu, J.-T.; Li, P.-J.; Yu, Z.-F.; Li, P. Petrology and spectroscopy studies on Danxia Geohéritage in Southeast Sichuan Area, China: Implications for Danxia surveying and monitoring. *Geoheritage* **2015**, *7*, 307–318. [[CrossRef](#)]
6. Babu, P.S.; Majumdar, T.J.; Bhattacharya, A.K. Study of spectral signatures for exploration of Bauxite ore deposits in Panchpatmali, India. *Geocarto Int.* **2015**, *30*, 545–559. [[CrossRef](#)]
7. Boesche, N.K.; Rogass, C.; Lubitz, C.; Brell, M.; Herrmann, S.; Mielke, C.; Tonn, S.; Appelt, O.; Altenberger, U.; Kaufmann, H. Hyperspectral REE (Rare Earth Element) mapping of outcrops—Applications for neodymium detection. *Remote Sens.* **2015**, *7*, 5160–5186. [[CrossRef](#)]
8. Qiu, J.-T.; Zhang, C.; Hu, X. Integration of concentration-area fractal modeling and spectral angle mapper for ferric iron alteration mapping and uranium exploration in the Xiemisitan Area, NW China. *Remote Sens.* **2015**, *7*, 13878–13894. [[CrossRef](#)]
9. Nair, A.M.; Mathew, G. Effect of bulk chemistry in the spectral variability of igneous rocks in VIS-NIR region: Implications to remote compositional mapping. *Int. J. Appl. Earth Obs. Geoinf.* **2014**, *30*, 227–237. [[CrossRef](#)]
10. Martini, J.E.J.; Bowles, M. *Metallogenic Map of the Republic of Congo, Scale 1:1,000,000*; Republic of Congo Ministry of Mines and Energy: Brazzaville, Congo, 1994.
11. Clark, R.N.; Swayze, G.A.; Gallagher, A.J.; King, T.V.V.; Calvin, W.M. *The U.S. Geological Survey, Digital Spectral Library: Version 1: 0.2 to 3.0 Microns*; U.S. Geological Survey Open File Report (No.93-592); U.S. Geological Survey: Reston, VA, USA, 1993; p. 1340.
12. Hunt, G.R.; Salisbury, J.W.; Lenhoff, C.J. Visible and near-infrared spectra of minerals and rocks: V. Halides, phosphates, arsenates, vanadates and borates. *Mod. Geol.* **1972**, *3*, 121–132.
13. Clark, R.N. Spectroscopy of rocks and minerals, and principles of spectroscopy. In *Manual of Remote Sensing*; Rencz, A.N., Ed.; John Wiley and Sons: New York, NY, USA, 1999; Volume 3, pp. 3–58.



© 2016 by the authors; licensee MDPI, Basel, Switzerland. This article is an open access article distributed under the terms and conditions of the Creative Commons Attribution (CC-BY) license (<http://creativecommons.org/licenses/by/4.0/>).